LAUTECH Journal of Engineering and Technology 2011 7 (1) : 1-5

MEASUREMENT OF MEAN VELOCITY PROFILE IN A TURBULENT PIPE FLOW – A NUMERICAL APPROACH

G.A Odewole[1], M.A. Waheed[2] and O.S. Olaoye[3,*]

[1]*School of Mechanical, Aerospace and Civil Engineering*
The University of Manchester, Manchester, United Kingdom

[2]*Department of Mechanical Engineering, College of Engineering*
University of Agriculture, Abeokuta, Nigeria

[3]*Department of Mechanical Engineering, Faculty of Engineering and Technology Ladoke Akintola University of Technology, Ogbomoso, Nigeria* * **Author for Correspondence**: segunolaoye2002@yahoo.co.uk, +234 (0) 803 8645 736

ABSTRACT
Computational Fluid Dynamics FLUENT codes were employed in the measurement of the mean velocity profile of a fully-developed pipe flow. The codes used the standard two equation eddy-viscosity ($k-\varepsilon$) model for analysing turbulence in the flow. Deviations of about 2-12%, 1.1-1.7% and 1.02-5.3% obtained between the numerical results and the experimental benchmark for the study in the viscous sub-layer, buffer region and the fully-developed region of the flow show the close agreements between the experimental and the numerical results.

Keywords: Computational Fluid Dynamics, Velocity Profile, Viscosity, Turbulence

DOI: https://doi.org/10.54043/laujet.2011.07.01.01

INTRODUCTION

Well-developed pipe flow profile at measurement positions is required for idealizing the measurement performance of conventional flow meters in the industries. This requirement, which may be in the form of long and straight length of constant-diameter pipe upstream of the measurement points, is important in overcoming the difficulties associated with such measurement.

Whilst the application of the Ultrasonic Velocity Profile (UVP), the Particle Image Velocimetry (PIV) and other measurement techniques has been successful in obtaining the mean velocity profile and Reynolds stress for single-phase laminar, transitional and turbulent flows in pipes and channels (Mori et al, 2002; Yamanaka et al, 2002; van Doorne and Westerweel, 2007; Bai et al, 2010; Odewole et al, 2010), the integrity of these results for application in a wider range of flow measurements are still questionable.

This paper therefore focuses on the use of the standard $k-\varepsilon$ model available in general-purpose Computational Fluid Dynamics (CFD) FLUENT codes, to estimate the velocity profile in a turbulent pipe flow using the measurement data of Odewole et al, 2010 as an experimental benchmark.

METHODOLOGY

Grid Size and Sensitivity

In order to allow a comparison with the experimental results of Odewole et al, 2010; numerical simulations are carried out on a two dimensional pipe model with a dimension of 102mm x 8976mm, with the dimension of the pipe sufficiently long enough to make the flow fully developed. The flow domain in this study is discretized into 16,800 mesh elements, with a greater mesh density placed in the vicinity of the pipe walls since the reliability of numerical results for wall-bounded flows depends on the grid resolution in the wall regions (Fluent, 2006).

The greater mesh density employed in the near-wall regions of the flow pipe for this study is also particularly important in order to obtain accurate information since the numerical results are susceptible to grid dependency in these regions.

Turbulence Model

The Navier-Stokes equations governing the incompressible, turbulent pipe flow in this study are solved by employing the Reynolds average technique of flow computation since direct numerical simulation places excessive demands on computational resources (time and space) for practical engineering analyses

(Rodgers and Eveloy, 2004). The Reynolds-Averaged Navier-Stokes (RANS) equations shown in Equations (1) and (2) are therefore combined with the standard $k-\varepsilon$ turbulence model in order to obtain accurate information on the flow. Equation (1) is for the conservation of mass while Equation (2) is the momentum equation in the *x*-, *y*-, and *z*-directions.

Viscous dissipation and radiation are not considered here.

$$\frac{\partial}{\partial x_i}\left(\rho u_i\right)=0, \qquad (1)$$

$$\frac{\partial}{\partial x_j}\left(\rho u_i u_j\right)=-\frac{\partial P}{\partial x_i}+\frac{\partial}{\partial x_j}\left[\mu\left(\frac{\partial u_i}{\partial x_j}+\frac{\partial u_j}{\partial x_i}-\frac{2}{3}\delta_{ij}\frac{\partial u_l}{\partial x_l}\right)\right]+\frac{\partial}{\partial x_j}\left(-\rho\overline{u_i' u_j'}\right). \qquad (2)$$

The need for turbulence modelling, in addition to solving the RANS equations above has grown tremendously over the years. This is as a result of the need to capture the different sizes of turbulent eddies, responsible for the transport and mixing of turbulence in fluid flow, on an appropriate scale. The Reynolds stress, $-\rho\overline{u_i' u_j'}$ in Equation (2) must be properly modelled for closure of Equations (1) and (2). The form of closure obtained depends on the type of turbulence model used. Using the two equation $k-\varepsilon$ model, $-\rho\overline{u_i' u_j'}$ can be related to the mean velocity gradients within the pipe using the Boussinesq approach as shown in Equation (3) (Versteeg and Malalasekera, 1995).

$$-\rho\overline{u_i' u_j'}=\mu_t\left(\frac{\partial u_i}{\partial x_j}+\frac{\partial u_j}{\partial x_i}\right)-\frac{2}{3}\left(\rho k+\mu_t\frac{\partial u_k}{\partial x_k}\right)\delta_{ij}. \qquad (3)$$

The advantage of the Boussinesq approach lies in the relatively low computational cost associated with the evaluation of the turbulent viscosity, μ_t (Rodgers and Eveloy, 2004; Fluent, 2006). With the $k-\varepsilon$ turbulence model, two additional equations for the turbulent kinetic energy, k and the turbulent dissipation rate, ε are solved.

$$\frac{\partial}{\partial x_i}\left(\rho k u_i\right)=\frac{\partial}{\partial x_j}\left[\left(\mu+\frac{\mu_t}{\sigma_k}\right)\frac{\partial k}{\partial x_j}\right]+G_k+G_b-\rho\varepsilon. \qquad (4)$$

$$\frac{\partial}{\partial x_i}\left(\rho\varepsilon u_i\right)=\frac{\partial}{\partial x_j}\left[\left(\mu+\frac{\mu_t}{\sigma_\varepsilon}\right)\frac{\partial\varepsilon}{\partial x_j}\right]+C_{1\varepsilon}\frac{\varepsilon}{k}\left(G_k+C_{3\varepsilon}G_b\right)-C_{2\varepsilon}\rho\frac{\varepsilon^2}{k}. \qquad (5)$$

The $k-\varepsilon$ turbulence model, since its introduction by Launder and Spalding (1974), has found extensive use in industries because of their modest requirements for computing resources, robustness, and their performance in obtaining fairly accurate predictions in most flows. Further readings and information on the $k-\varepsilon$ model can be obtained from the following literatures: Nallasamy, (1987); Menter, (1994) and Fluent, 2006.

Numerical Method

The discretized forms of the RANS equations in (1) – (3) above and Equations (4) and (5) for the turbulence employed in this study were solved on a control-volume basis using a pressure-based solver, where a segregated solution algorithm was used. The momentum and other scalar variables constituting the convection terms on the cell faces of Equations (1) – (5) were obtained using the second order upwind scheme in order to reduce numerical diffusion while the second-order accurate central-differencing scheme was employed for the diffusion terms of the governing equations.

Since FLUENT adopts a co-located scheme, where pressure and velocity values are both stored at centres of computational cells, it therefore implies that cell-centred pressure values also have to be interpolated to obtain pressure values at the face of cells. To do this, the second order pressure interpolation scheme was adopted. In order to model the interaction between pressure and velocity, pressure correction was carried out on Equation (1) so as to couple together pressure and velocity values in Equations (1) and (2) using the SIMPLE (Semi-Implicit Method for Pressure-Linked Equations) algorithm for pressure-velocity coupling described by Patankar (1980).

Using the size of the flow inlet as a dominant length scale in the description of the flow regime in a non-dimensional form, a Reynolds number of 6800 was used as the basis for the selection of the appropriate turbulence model à priori. Consequently, the two-equation, eddy-viscosity model ($k-\varepsilon$) was then used for modelling turbulence in the pipe flow. In order to bridge the viscosity-affected near-wall region and the fully turbulent core of the pipe together, a two-layer based, non-equilibrium wall function was used. This wall function sensitized the Launder and Spalding's logarithmic law for mean velocity to pressure-gradient effects in the flow (Launder and Spalding, 1972).

The kinetic energy of turbulence in near-wall cells is computed based on the assumption that the flow in the pipe can be regarded as made of a viscosity-affected near-wall region and the fully turbulent core. Thus, the use of the non-equilibrium wall functions effectively relaxes the local equilibrium assumption adopted by the standard wall functions in computing the budget of kinetic energy of turbulence at near-wall cells (Menter, 1994 and Nallasamy, 1987). Convergence of the steady, incompressible turbulent pipe flow was checked by ensuring that the scaled residual, R^{ϕ} in Equation (6) below, is less than 10^{-4} for all variables. User modifications, where applicable, were made to the implementation of the turbulence model employed in the FLUENT code.

$$R^{\phi} = \frac{\sum_{cells,C}\left|\sum_{nb} a_{nb}\phi_{nb} + b_{o} - a_{C}\phi_{C}\right|}{\sum_{cells,C}\left|a_{C}\phi_{C}\right|} \quad . \qquad (6)$$

RESULTS AND DISCUSSION

A comparison between the mean velocity profiles obtained from the numerical measurement carried out in this study and the experimental data of Odewole et al, 2010 is depicted in Figure 1 below. It is evident from Table 1 that a good agreement exists between the experimental and the numerical data in the viscosity-affected inner layer of the pipe since a deviation of about 2-12% is obtained. This viscosity-affected inner layer, where the viscous force predominates the inertia force, lies between y = 0 (the wall of the pipe) and a distance y = 0.41mm away from the wall, where y is measured in wall units.

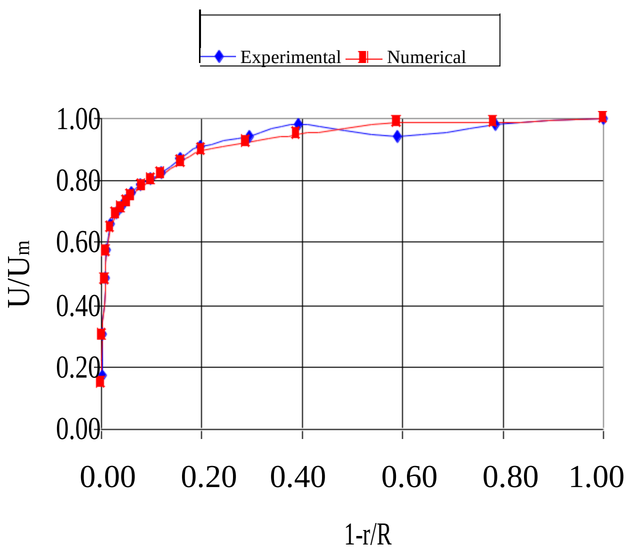

Figure 1: Comparison of Linear Velocity Profiles

Table 1: Mean Velocity Profile Measurements

Experimental Measurement (Odewole et al, 2010)		Numerical Measurement (Present Study)		Deviation
U/U_m	1-r/R	U/U_m	1-r/R	(%)
0.17	0.0020	0.15	0.0000	11.76471
0.31	0.0039	0.30	0.0040	3.225806
0.49	0.0078	0.48	0.0080	2.040816
0.58	0.0118	0.57	0.0120	1.724138
0.66	0.0196	0.65	0.0200	1.515152
0.70	0.0294	0.69	0.0300	1.428571
0.72	0.0392	0.71	0.0400	1.388889
0.74	0.0490	0.73	0.0500	1.351351
0.76	0.0588	0.75	0.0600	1.315789
0.79	0.0784	0.78	0.0800	1.265823
0.81	0.0980	0.80	0.1000	1.234568
0.83	0.1176	0.82	0.1200	1.204819
0.87	0.1569	0.86	0.1600	1.149425
0.91	0.1961	0.90	0.2000	1.098901
0.94	0.2941	0.92	0.2900	2.12766
0.98	0.3922	0.95	0.3900	3.061224
0.94	0.5882	0.99	0.5900	-5.31915
0.98	0.7843	0.99	0.7800	-1.02041
1.00	1.0000	1.00	1.0000	0

Whilst the CFD codes can predict accurately the velocity variation in the flow within this region, the inability of the hot-wire probe employed in the experimental measurement of the velocity profile in obtaining a good fit of data for the velocity variation within this region lies in the geometry of the hot-wire probe. The pre-calibrated straight hot-wire probe is unable to reach the wall of the pipe, with the measurement of the velocity profile starting at a distance corresponding to y = 10mm from the wall. This causes restricted data for the velocity variation within the viscosity-affected inner layer of the pipe to be obtained. Further information on the experimental procedure and measurement can be obtained from Odewole et al, 2010. However, a higher mesh density positioned at the wall and within the vicinity of the wall ensures that adequate information for the velocity variation within the viscosity-affected inner layer can be obtained from the numerical investigations.

A very good agreement is also obtained between the experimental and numerical data in the buffer region of the flow where the turbulent eddies are rapidly damped and consequently, the turbulent shear stress is reduced to practically zero levels in comparison to the viscous stress. This zone, corresponding to the region between y = 0.61mm to y = 10.2mm in Figure 1, shows a deviation of 1.1-1.7%. Beyond the buffer region, the contribution of viscosity decreases till equal contribution is obtained between the viscous and the inertia forces in the flow. This region, corresponding to y = 10.2mm and y =

51mm (the centreline of the pipe), is called the fully-developed region of the flow. A maximum deviation of about 5.3% exists between the experimental and the numerical data in this region.

CONCLUSION

In this paper, the velocity profile of a turbulent pipe flow has been measured numerically using FLUENT while turbulence in the pipe flow was modelled using the standard $k-\varepsilon$ model as a result of its robustness in promoting stable convergence and universality for most practical engineering analyses. Deviations of about 2-12%, 1.1-1.7% and 1.02-5.3% obtained in the viscosity-affected inner layer, buffer region and the fully-developed region of the pipe flow in comparison with the experimental results are evidence of the close agreements between the numerical results and the experimental benchmark employed for the study. An alternative method of measuring the velocity profile of conventional flow meters is therefore provided by the results of this numerical study. Using this measurement technique, savings in cost and time are obtained without the need for recourse to experimental measurement techniques requiring high capital outlay.

AKNOWLEDGEMENT

The authors greatly acknowledge The University of Manchester, UK for permission to use FLUENT for this numerical study.

REFERENCES

Bai, H.L., Li, W.J., Chow, W., Zhou, Y. (2010). A carbon nanotube sensor for wall shear stress measurement. Experiments in Fluids, Vol. 48, pp. 679-691.

Fluent6.3 User's Guide (2006). Fluent Inc., 10 Cavendish Court, Lebanon, NH 03766.

Launder, B.E. and Spalding, D.B. (1972). Mathematical Models of Turbulence. Academic Press Inc., London, ISBN 0-12-438050-6.

Launder, B.E., Spalding, D.B. (1974). The Numerical Computation of Turbulent Flows. Computer Methods in Applied Mechanics and Engineering, Vol. 3, pp. 269-289.

Menter, F.R. (1994). Eddy Viscosity Transport Equations and their Relation to the $k-\varepsilon$ Model. NASA Technical Memorandum 108854, pp. 1-24.

Mori, M., Takeda, Y., Taishi, T., Furuichi, N., Aritomi, M., Kikura, H. (2002). Development of a novel flow metering system using ultrasonic velocity profile measurement. Experiments in Fluids, Vol. 32, pp. 153-160.

Nallasamy, M. (1987). Turbulence Models and their Applications to the Prediction of Internal Flows: A Review. Computers and Fluids, Vol. 15, No. 2, pp. 151-194.

Odewole, G.A., Waheed, M.A., Olaoye, O.S. (2010). Measurement of mean velocity and Reynolds stress profiles in a turbulent pipe flow. Science Focus, Vol. 15, Issue 2, pp. 236-248.

Patankar, S.V. (1980). Numerical Heat Transfer and Fluid Flow, Hemisphere, ISBN 0-89116-522-3, Washington, DC.

Rodgers, P., Eveloy, V. (2004). Application of low-Reynolds number turbulent flow models to the prediction of electronic component heat transfer. Proc. of the 9th Intersociety Conf. on Thermal and Thermomechanical Phenomena in Electronics Systems, pp. 495-583.

van Doorne, C.W.H., Westerweel, J. (2007). Measurement of laminar, transitional and turbulent pipe flow using stereoscopic-PIV. Experiments in Fluids, Vol. 42, pp. 259-279.

Versteeg, H.K. and Malalasekera, W. (1995). An Introduction to Computation Fluid Dynamics: The Finite Volume Method. Pearson Education Ltd, ISBN 0-582-21884-5, England.

Yamanaka, G., Kikura, H., Takeda, Y., Aritomi, M. (2002). Flow measurement on an oscillating pipe flow neat the entrance using the UVP method. Experiments in Fluids, Vol. 32, pp. 212-220.

NOMENCLATURE

General

Quantity	Description	Unit
x_i, x_j, x_k, x_l	Coordinate axes	-
u_i, u_j, u_k, u_l	Mean velocity components	ms^{-1}
u_i', u'_j	Fluctuating velocity components	ms^{-1}
P	Fluid pressure	Nm^{-2}
k	Turbulence kinetic energy	m^2s^{-2}
a	Equation coefficient	-
b_o	Net source term	-
G_k	Generation of turbulent kinetic energy due to mean velocity gradients	$kgm^{-3}s^{-3}$
G_b	Generation of turbulent kinetic energy due to	$kgm^{-1}s^{-3}$

	buoyancy	
$C_{1\varepsilon}$, $C_{2\varepsilon}$, $C_{3\varepsilon}$	Empirical constants	-
R^{ϕ}	Convergence indicator	-

Greek Letters

Quantity	Description	Unit
ρ	Fluid density	kgm^{-3}
μ, μ_t	Dynamic and turbulent viscosities	$kgm^{-1}s^{-1}$
δ_{ij}	Kronecker delta	-
ε	Turbulence dissipation rate	m^2s^{-3}
ϕ	Transport scalar variable	-
σ_k, σ_ε	Turbulent Prandtl numbers for k and ε	-

Dimensionless Quantities

Quantity	Description	Unit
$Re(=\rho uD/\mu)$	Reynolds number	-

Subscripts

Quantity	Description	Unit
nb	Neighbour cells	-
C	Central node on control volume	-
$cells$	Control volumes	-